Half-wet nanomechanical sensors for cellular dynamics investigations

Martina Conti [ab], Laura Andolfi [b], Erik Betz-Güttner [ab], Simone Dal Zilio [b] and Marco Lazzarino[b]

[a] *University of Trieste, Department of Physics, PhD in Nanotechnology, 34100 Trieste, Italy*

[b] *CNR-IOM, Istituto Officina dei Materiali - Consiglio Nazionale delle Ricerche, 34149 Trieste, Italy*

Abstract

Testing devices based on cell tracking are particularly interesting as diagnostic tools in medicine for antibiotics susceptibility testing and *in vitro* chemotherapeutic screening.

In this framework, the application of nanomechanical sensors has attracted much attention, although some crucial aspects such as the effects of the viscous damping, when operating in physiological conditions environment, still need to be properly solved. To address this problem, we have designed and fabricated a nanomechanical force sensor that operates at the interface between liquid and air.

Our sensor consists of a silicon chip including a 500 μm wide Si_3N_4 suspended membrane where three rectangular silicon nitride cantilevers are defined by a lithographically etched gap. The cantilevers can be operated in air, fully immersed in a liquid environment and in half wetting condition, with one side in contact with the solution and the opposite one in air. The formation of a water meniscus in the gap prevents the leakage of medium to the opposite side, which remained dry and is used to reflect a laser to measure the cantilever deflection. This configuration enables to keep the cells in physiological environment while operating the sensor in dry conditions.

The performance of the sensor has been applied to monitor the motion and measures the forces developed by migrating breast cancer cell. The functionalization of one side of the cantilever and the use of a purposely designed chamber of measurements enable the confinement of the cell only on one side of the cantilever.

Our data demonstrate that this approach can distinguish the adhesion and contraction forces developed by different cell lines and may represents valuable tool for a fast and quantitative *in-vitro* screening of new chemotherapeutic drugs targeting cancer cell adhesion and motility.

Keywords

Atomic force microscopy; Nanomotion; Nano-mechanical sensor, Biosensors; Cantilever sensor.

Introduction

Micro-mechanical cantilevers, developed as the sensing part of an Atomic Force Microscope (AFM), demonstrated promising applications also as independent sensors, thanks to their capability of measuring the change of surface stress, adsorbed mass and heat dispersion. Originally focused on material science [1] have been extended to biology, medicine and clinical diagnostic applications [2,3].

Recently, a novel application for microcantilevers called AFM-nanomotion detection has been proposed [4]. This technique allows detecting nanometric scale oscillations of living cells attached on commercial cantilevers. Their presence on the cantilever surface induces dynamic deformations which can be recorded in time. The time evolution of this motion can be further correlated with the viability and metabolic state of living specimens [5]. Nanoscale vibrations have been observed for different cells like bacteria [6], plant and mammalian cells [4]. Although this technique represents major advance in the direction of a label-free, sensitive and fast method to detect the motion of living cells [7–9], it suffers from several important limitations.

Commercial cantilevers when used as biological sensors are typically soaked in a physiological, mostly a water-based, medium. This condition does not affect significantly their response when operated in static mode, for instance measuring the deflection induced by a molecular reaction occurring at the cantilever surface [10], but it becomes a serious limitation when they are operating in dynamic mode. For instance, the molecular mass deposited on a cantilever can be evaluated by measuring its resonance frequency variation; in this case, the viscous damping of the medium significantly broadens the frequency response and reduces the frequency shift sensitivity [11].

A first attempt of minimizing the effect of liquid immersion was proposed by Melli et al. [12], who used a superhydrophobic surface to limit the sensor interaction with the biological solution, but still detected the mass variation in vacuum. A very sophisticated alternative was proposed by Manalis group [13] who, with an abrupt change of perspective, moved the liquid environment

inside the cantilever, fabricating an oscillating microfluidic channel. A simpler, and most effective approach, was proposed by Oesterschulze's group who demonstrated that, by a suitable geometry, it is possible to put only one side of a cantilever in contact with the liquid, while maintaining the resonance performance of air operation [14,15]. Further drawbacks of fully soaked cantilevers include the presence of refraction index inhomogeneities, liquid turbulence or the presence of cell debris which could further affect the system response.

Furthermore, any kind of biosensors must be functionalized with appropriate molecules to facilitate cell interactions or adhesion. Such procedure, when applied to fully immersed cantilevers, generally creates a coating on all the exposed surfaces [10,11], resulting in cells grown on both cantilever sides. As a consequence, both the presence of cells on the back side, where laser is focused, can interfere with laser deflection, and cellular forces are applied on opposite sides, which could balance each other, providing misleading results.

Finally, since the liquid environment operation makes the cells mass measurement very difficult due to the poor-quality factor of the sensor, the mass measurements must be performed in air after fixation, and mass evolution in physiological process such as cell growth and replication cannot be investigated.

To overcome all these limitations, we propose a novel sensor called *half-wet nanomechanical* (HWN) *sensor*, which, thanks to its peculiar design, can operate in half wetting condition. In this work we characterise the mechanical features of the sensor and we demonstrate the ability of the HWN sensors to detect the motility and the forces developed by different breast cancer cells during adhesion and motion process.

Materials and Methods

Design and fabrication of HWN sensor

To explore a wide range of mechanical forces, suspended microcantilever with three different lengths 50 µm, 100 µm and 200 µm, and 30 µm of width were fabricated (Fig. 1a). The chips with suspended cantilevers were fabricated using conventional micromachining approach and started from a 500 µm thick silicon wafer coated on both sides with a 2 µm thick low-stress LPCVD silicon nitride (Si_3N_4).

At first, a 150nm thick chromium film was deposited on both sides by DC magnetron sputtering; a positive photoresist (MEGAPOSIT™ SPR™220 1.2) was spin-coated at 3500 rpm for 45 seconds on both sides and pre-baked at 115°C for 1 minutes and 30 seconds; a double-sided aligned exposure by standard proximity UV lithography using two masks allow the resist patterning: the upper mask contains the cantilevers pattern while the lower mask the structures for the windows definition. After resist development, the pattern was transferred into the chromium film by wet etching process, in a mixture of water, acetic acid (CH_3COOH), and ceric nitrate ammonium $(CeNH_4)_2 (NO_3)_6$. Then the exposed Si_3N_4 was dry etched: for the windows structures, by reactive ion etching (RIE) using a mixture of CF_4/O_2 (150W, 100V bias); for the cantilever by inductively coupled plasma RIE (ICP-RIE), using a mixture of $SF_6/C_4F_8/O_2$ (240W, 50V bias). The Si_3N_4 cantilever were released by wet etching in KOH solution (30 wt %, 80°C). In the following, the Si_3N_4 surface that was previously in contact with the bulk silicon wafer will be referred as the "laser-side", while the opposite surface will be referred as the "cell-side". Finally, the chromium mask was removed in etchant solution. The chip with the suspended cantilevers were characterized by scanning electron microscopy (SEM) (Fig. 1b, c).

We fabricated and tested gaps with different width (2, 4, and 8 µm) surrounding the cantilevers for the optimization of the half wetting condition, such as to reduce the solution leakage through the cantilever gap (the wider the gap higher the leakage probability) and minimize the meniscus elastic response (the narrower the gap the stiffest the meniscus response).

The chips were further cleaned in O_2 plasma oxygen (1 min, 40 W, Bias 100 V) and coated with a Ti-20nm – 50nm Au thin film on the back side to improve the laser reflectivity.

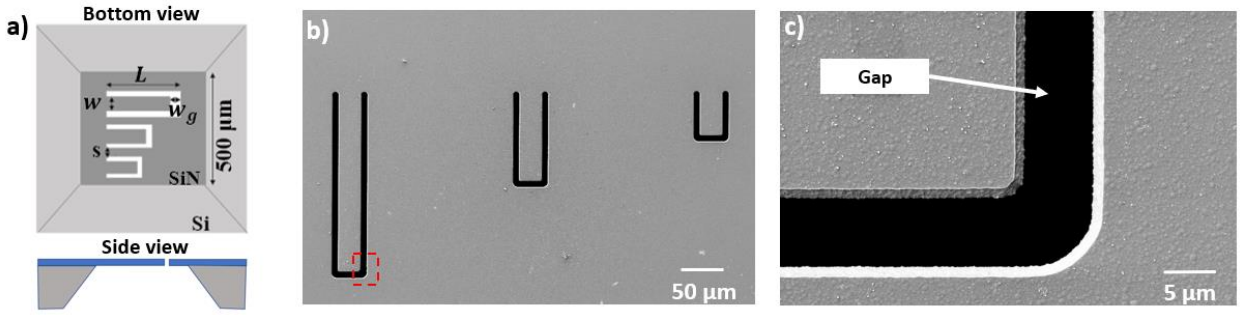

Figure 1: Cantilever geometry *a) Schematic diagram of bottom and side view of suspended cantilevers; SEM image of a suspended cantilever array etched on* $\boldsymbol{Si_3N_4}$ *membrane: b) Cantilevers with a width of 30 µm, a gap of 4 µm, and 200 µm, 100 µm and 50 µm long, respectively; c) Magnified view of the area indicated by a red square in (b) to highlight the area of the gap, as indicated by the white arrow.*

F*unctionalization of the cantilevers*

The HWN sensor surface was functionalized with a 3-amino-propyl-triesthoxysilane (APTES) monolayer, an aminosilane commonly employed in biosensors applications that creates a monolayer, which facilitates cell adhesion by exposing amino groups on the surface, as demonstrated by several studies [18–22].

Often APTES-based treatments is performed in solution resulting in the functionalization of both sides of the cantilever [5,6]. We use an alternative protocol based on vapor phase deposition, as described in literature [23,24], to functionalize only the cell side of the sensor, while keeping the laser side of the cantilever free from contaminant that can affect laser reflectivity. Such a functionalization protocol was used to develop a low-cost CMD-based patterned surface for biosensing applications.

In detail, the chips with the laser side facing downwards were attached on a silicon substrate using a Kapton tape and then underwent to plasma O_2 process (1 min, 40W, 100 bias), both to clean the substrate and to expose the silanol groups on the surface for the following functionalization process. A glass Petri dish filled with 300 µl of APTES was placed on the bottom of a glass vacuum chamber maintained at 10^{-3} - 10^{-5} mbar, and warmed at 50°C. The sample was mounted upside down 20 cm above the Petri dish and exposed to APTES vapour for 4 hours, and then further annealed for two hours at 120°C in a separated vacuum oven.

The cantilever functionalization was verified by contact angle (CA) measurements (Fig. S1) carried out on a DataPhysics OCA 15Pro optical instrument (DataPhysics Instruments GmbH, Germany) by placing 2 µL of Milli-Q water onto Si_3N_4 surfaces before and after functionalization process at ambient temperature. The average CA values were obtained by averaging over four different positions on three samples. We measured (79 ± 3) ° for Si_3N_4 surface one hour after the APTES deposition process.

Calibration of cantilever

The spring constant of the fabricated cantilevers was calculated using a rectangular commercial cantilever NSC18/AIBS (μMasch) as reference probe, with comparable length, width and thickness, whose spring constant was previously evaluated by the thermal noise procedure [25,26]. To perform the measurement, the reference probe was mounted on the AFM-tip holder and the cantilever to be evaluated was fixed on glass coverslip with double-sided tape. A sketch and explanation of the calibration procedure is displayed in Fig. S2. Finally, to convert the cantilever deflection into force, we evaluate the cantilever sensitivity using the non-contact approach of the JPK- NanoWizard III AFM software based on Sader's theory, which does not require the acquisition of a force-distance curve on a hard surface. This method allows to obtain the inverse optical lever sensitivity (InvOLS) of the rectangular cantilevers from the thermal spectrum [27,28].

Chamber of measurements

To test the HWN sensors, we designed and fabricated a measurement chamber (Fig. 2) that can be used on an inverted microscope to perform fluorescence optical microscopy and is compatible with the head of a JPK-NanoWizard II and Nanowizard 3 AFMs so that the embedded laser detection system can be used to measure the resonant frequency and deflection of the HWN sensor cantilevers. The chamber of measurements consists of a circular holder for mounting the chip (with "laser side" faced up) (Fig. 2a), and two metal rings with screws to seal the holder, which is then inserted into a Petri dish lid (Fig. 2b). After sealing, the resulting chamber of measurements (Fig. 2c) is placed under the head of the AFM to perform experiments (Fig. 2d). For the experiments with living cells, as indicated by the red arrows, the holder is turned upside-down after chip mounting (with the "cell side" of the chip faced up) and placed into a Petri dish to perform the cell seeding. After seeding, the holder is sealed by a metal ring with the "laser side" facing up, and then inserted into the AFM.

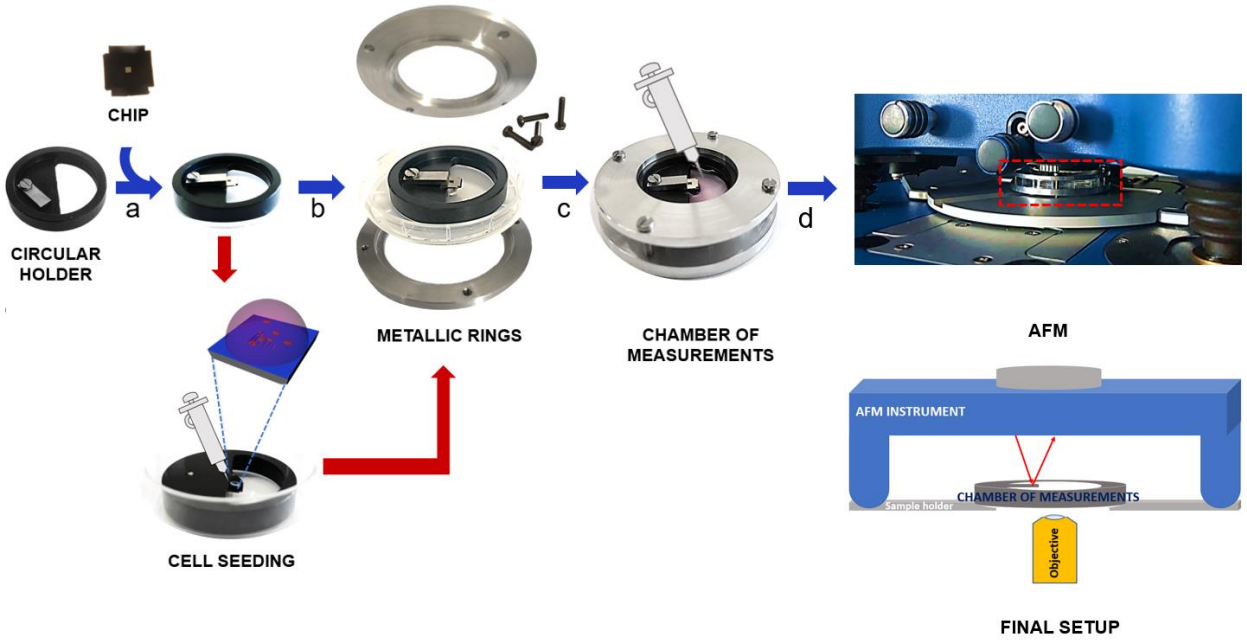

Figure 2: Chamber of measurements and chip mounting. *a) the chip with the fabricated cantilevers is mounted on a circular holder with the "laser side" facing up; b) after mounting the chip, the circular holder is placed on a Petri dish lid held with a thin PDMS foil (25 µm thick); c) then the circular holder and Petri dish lid are sealed with metal rings to create a measurement chamber and then filled with the liquid; d) finally, the sealed chamber (dashed) is inserted into the JPK-NanoWizard II AFM to perform the measurements. In the bottom right corner, a scheme of the setup in the measuring configuration is displayed: the chamber of measurement is placed on the microscope "sample holder", under the head of the AFM. The objective of the inverted microscope is located under the sample holder and is used to visualize the "cell side" of the chip (faced down). As shown by the red arrows in the figure, for the experiments with living cells, after mounting the chip, the holder is placed in a Petri dish with the "cell side" faced up and the cell seeding is performed: a 25 µl droplet of cells is placed on the "cell side" of the chip and kept in the incubator (37°C and 5% CO2) for 20 minutes to allow the cells to adhere, while the laser side (facing down) is kept dry. The holder is then turned upside down, placed on the lid of a Petri dish and sealed with the metal rings. The resulting measurement chamber is filled with the liquid (650 µl final volume to ensure the half-wetting condition).*

Resonance frequency measurements of cantilevers

The cantilever resonance frequency measure was obtained using a home-built photothermal excitation system, integrated into a JPK- NanoWizard II AFM in three different conditions: air, partial and fully wet in milliQ water. In detail, the chip with suspended cantilevers was mounted on a home-made circular holder, which was then inserted into a Petri dish lid to obtain a chamber for measurements (Fig. 2). The excitation laser (375 nm, 70 mW) was focused on the laser side the cantilever at the fixed end, while the detection laser was focused on the laser side at the free end of the cantilever and then aligned on the AFM photodiode detector. For the half-wet condition, the fluid chamber was filled with 650 µl milliQ water, while for the fully wet condition, the chamber was completely filled so that the cantilever was completely immersed in the liquid.

Cells and cell-culture

MDA-MB-231 (ECACC 92020424) and MCF-7 (Sigma-Aldrich ECACC, #92020424) cells were cultured in a Dulbecco's modified eagle medium DMEM-high glucose, with L-glutamine and sodium pyruvate (Sigma-Aldrich), supplemented with 10% (v/v) of fetal bovine serum (FBS) (Sigma-Aldrich) and 1% (v/v) penicillin-streptomycin (EuroClone) at 37°C 5% of CO2 incubator.

Cell experiments with the *HWN sensor*

To use the HWN sensors to monitor the cell adhesion, spreading and motility, cells are grown on the cell-side while the backside, where the laser beam is focused, in kept dry. To this purpose we used a chamber of measurements purposely optimized to be compatible with both an inverted microscope and the JPK- NanoWizard II and Nanowizard 3 AFM laser detection system. As shown in Fig. 2 (red arrows), the holder with the chip is inserted into a Petri dish and a 25 µl drop containing about 3.000 cells is placed on the cell side of the chip (in sterile conditions) and incubated for 20 minutes in humidified atmosphere at 37°C and 5% CO_2 to allow cells to adhere, while the backside is kept dry. Afterward, the holder is turned upside-down placed on the Petri dish lid and sealed by metallic rings, thus creating a chamber of measurements which is filled with the medium (650 µl final volume) and placed under the head of an AFM. As result the cell-side of the cantilever with adherent cells is in contact with the medium, while the formation of a meniscus in the gaps allows to keep dry the backside, on which the laser beam of the AFM system is focused.

To count the cells adherent on the cantilever, a 25 µl drop of NucBlue (NucBlue™ Live ReadyProbes™) was added to the medium and incubated with the cells for 10 minutes before deflection measurements.

Fluorescence images and time lapse movies of the adherent cells were acquired on the inverted microscope Zeiss AxioVert200 with a 20X objective and XM10 camera (Olympus Corporation). The fluorescence images were acquired with 500 milliseconds exposure time, while in time lapse an image with 65 ms exposure time was acquired every 30 seconds for a total time of 15 minutes. Images were then analyzed in the ImageJ software.

Data acquisition and processing

The cantilever deflection was detected using "real-time" oscilloscope mode of NanoWizard II AFM (JPK Instrument, AG). The vertical deflection signal was collected at a sampling frequency of 1 kHz for 15 minutes. During the measurements, the temperature of the set-up was monitored and kept at $30^{o} \pm 1^{o}$ C. Before analysis, the thermal drift was subtracted from the data by linear flattening. The cantilever deflection of the resulting curves was then converted into force by using K and sensitivity evaluated as described previously.

To estimate the force developed by adherent cells on the cantilevers we analysed the macro and micro-oscillations of the deflection curves. First, we down sampled the data set of the curve (one point every 100) and then performed smoothing using the average of 500 neighboring points. In the resulting baseline curve, the peaks and minima are identified as macro-oscillations. Then the same baseline curve is subtracted from the data curve to obtain additional peaks and minima, which are identified as micro-oscillations (see Fig S3).

Analysis of the variance was obtained on the entire interval of measurements (15 minutes) (Supplementary section).

The moving variance was obtained by calculating a variance value for intervals of 100 milliseconds. Each value is plotted as function of time. All data processing and analysis were performed with Matlab R2019a and OriginPRO2021b software.

Results and discussions

Characteristics of cantilevers

In air the spring constant (k) of the suspended cantilever does not depend on the gap size, whereas in the half-wet condition (HW) the formation of the meniscus at the gap surrounding the cantilevers affects the k values of the cantilevers. To quantify this effect, the cantilevers were calibrated statically both in air and HW conditions. For the cantilevers 50 µm long we observe an extremely large variability of *k* values both in air and HW conditions, which likely results from the unprecise positioning of the AFM tip of the reference cantilever on the edge of the tested one, which is particularly relevant for the shorter ones. In air spring constant values of (25 ± 6) N/m and (3 ± 1) N/m were found for cantilevers of 100 µm and 200 µm long, respectively. When measured in HW condition, both cantilevers showed an increase of the measured k values, which was larger for smaller gap sizes. The increase of the k-values when moving from the in-air condition to the HW-condition was evaluated for each cantilever, and then the HW/AIR ratio was plotted (Fig. 3). For the smaller gaps (2 µm and 4 µm) the stiffening induced by the water meniscus is relevant, up to an average increase of 70% of the k values in the case of 2 µm gap and 200 µm long cantilevers. For the 8 µm gap, the meniscus contributes with a 10% to the stiffness value, without a significant difference between 100 µm and 200 µm length.

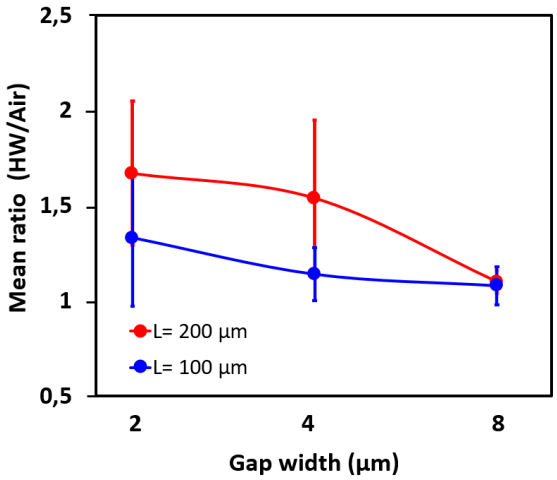

Figure 3: The air/water interface surface tension in HW increases the spring constant. *The mean HW/AIR ratio of spring constant values of the suspended cantilevers with different length as a function of the gap width.*

The resonance spectra obtained for the cantilevers of 100 µm and 200 µm long are shown in Fig.4. In air, resonance frequencies of 240 kHz and 64 kHz respectively were obtained. By fitting a Lorentzian function to these spectra, a quality factor (QF) of 66 and 116 was extracted, respectively. In HW condition, we observed a shift to lower resonance frequencies for both lengths, with peak values of 106 kHz and 30 kHz and a QF= 23 and 10.6 for cantilevers of 100 µm and 200 µm of length, respectively. In full-wet condition (FW), the resonance frequencies were 48.8 kHz and 24.1 kHz, with 5.4 and 1.7 QF. Operating in HW conditions induce a QF decrease of 3 and 10 times for 100 µm and 200 µm long cantilevers, which, although significant, still allow the application of cantilever as mass detectors. On the contrary, in FW condition the change in QF is dramatic, up to a factor 100 (Fig.4a, b). Hence the HW configuration drastically reduces the viscous damping, as also proposed by other authors [14].

The reduced impact on the quality factor is an important aspect also for improving mass detection in liquids for biological applications. As a proof of concept, we tested our HWN sensors for mass measurements of MDA-MB-231 breast cancer cells. The spectra acquired to for 200 µm long cantilever with a 4 µm gap size, before and after cell adhesion, are shown in Fig.4c. We observed a negative resonance shift of 1.3 kHz for the presence of 5 cells. Because the resonance frequency shift generally depends on the position of the cell on the cantilever and the surface tension applied to the cantilever by the cell adhesion and migration process [13,29–32], and living cells move continuously on the sensor surface, changing their position and the exerted forces from measurement to measurement, an accurate determination of the cell mass is not possible.

An estimate of the single-cell mass was made assuming a uniform distribution of cells along the cantilever and across the gaps. To determine the value of the resonant frequency, the frequency curves were fitted with Lorentzian functions. The corresponding values of the resonance peaks were used to calculate the additional mass due to the presence of cells in dynamic mode, as described in the literature [29,33]. The results showed an additional mass of 0.1 ng for the cantilever with 5 adherent cells. The value of mass was ~0.02 ng/cell. This value is about 10-100 times lower than the mass of single cells measured in the literature [33–35]. This result confirms that the stiffening contribution of the cells on the gaps affects the measure of mass.

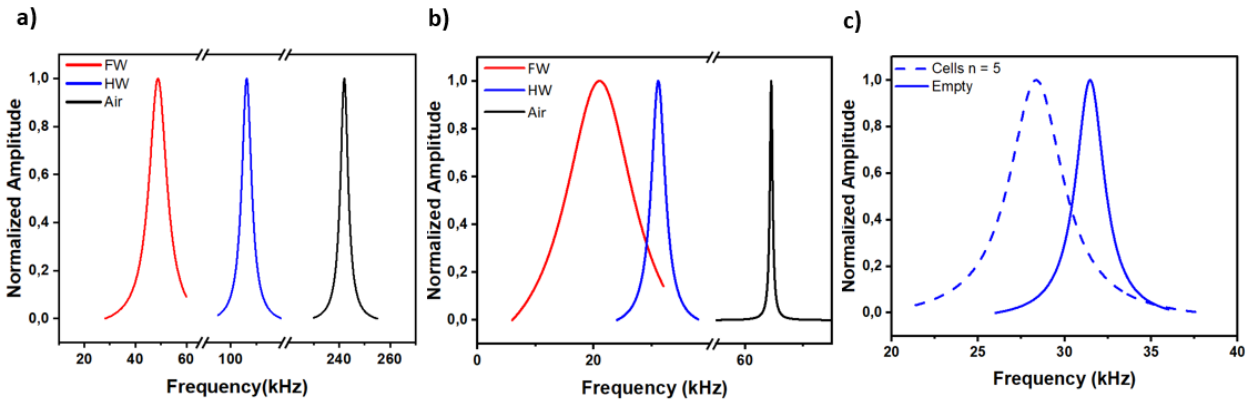

Figure 4: The resonance frequency and quality factor depend on the wetting condition and on the cell loading. *Resonance frequency of 100 μm (a) 200 μm (b) cantilevers long in air (black), half wetting (blue) and fully wetting (red) conditions; normalized amplitude value for empty cantilever (solid) and in presence (dash) of n=5 cells (c), as obtained in half-wetting condition.*

Measurements with HWN sensors

To investigate cell motility and adhesion force, we focused on cantilevers 200 µm long with a gap of 2 µm and 4 µm because the force sensitivity improves at lower spring constants [2]. The gap size of 8 µm was not suitable for these experiments, since we frequently observed that the cells somehow remained trapped in the gap, leading to a decrease in their motility.

The deflection curves acquired in the presence of cells can be converted into forces by using the values of *k* and s*ensitivity* obtained for the cantilever. We measured the deflection of the same cantilever before (Fig. 5a) and after (Fig. 5b) cell adhesion in HW (blue traces) and FW (red traces) conditions. In absence of cells the signal amplitude is larger in the FW conditions, indicating that the presence of the medium on the laser side perturbs the read-out adding an extra noise contribution. When cells are present on the cantilevers, the signal amplitude remains the same, but the deflection variation induced by the cell motion appear much larger on the cantilevers operated in HW conditions. Since cell behaviors on the cell side of the cantilever cannot be influenced by the presence or not of culture medium on the laser side, we can conclude that HW condition offer a much higher sensitivity to cell-induced deflection.

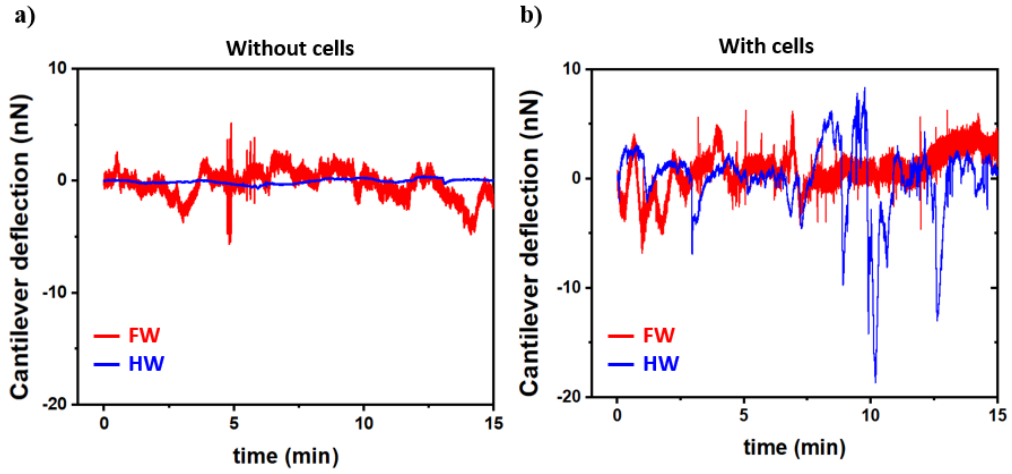

Figure 5: Half wetting condition increases the sensitivity to cell motion. *Deflection signal recorded in half wetting (blue) and in full wetting conditions (red) for the same cantilever in absence (a) and in presence (b) of MDA-MB-231 cells.*

To better assess the variation of the signal over time, we performed the moving variance analysis (Fig. 6). Due to the higher damping, the FW configuration was able to follow slow variations. In fact, the moving variance showed significant differences when the time interval for which the value is calculated is of the order of Q/f, i.e.,~60 msec and~300 msec for FW and HW, respectively. By using these values, the moving variance analysis showed that the difference between the cantilever before (without cells) and after cell adhesion (with cells) is less remarkable in FW condition (Fig. 6a) than in HW (Fig. 6b). Indeed, in FW the spurious peaks, likely due to cellular debris or other factors interfering with the laser path, complicate the interpretation of the signal after cell adhesion.

At longer time intervals of moving variance (3 seconds) we observed an increase in the values after cells adhesion in HW condition (Fig. 6c, blue traces), while in FW condition (Fig. 6c, red traces) a decrease in the variance signal, because of the higher damping, was observed. All together, these data confirm the highest sensitivity of the sensors operating in HW conditions.

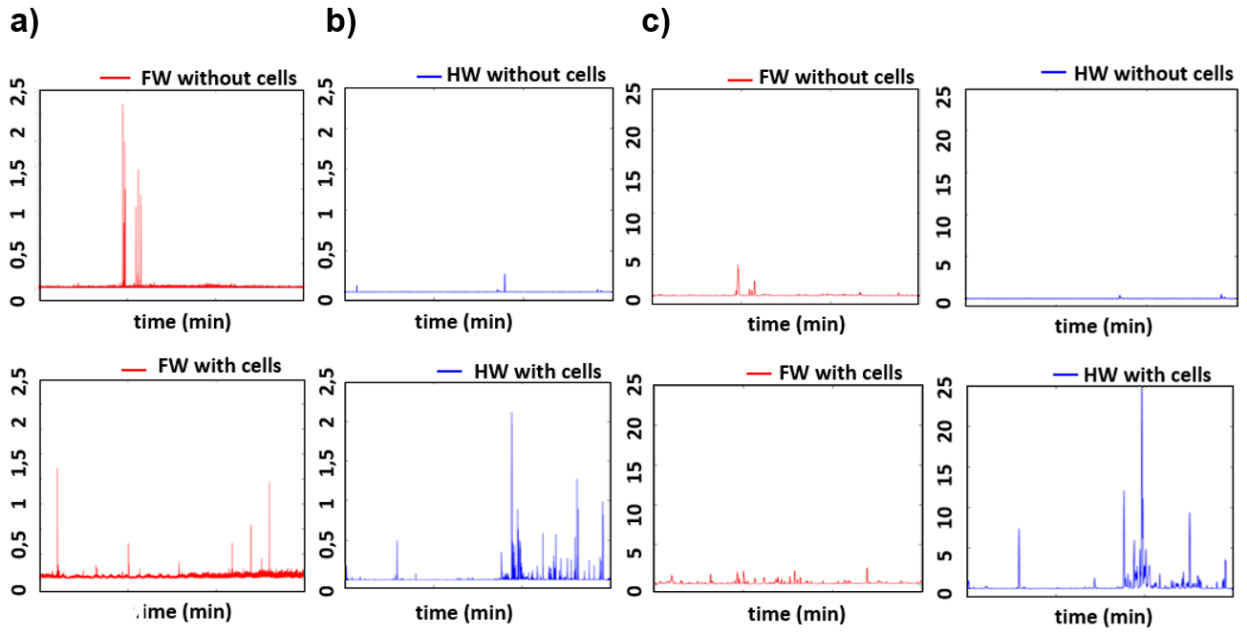

***Figure 6**: **The moving variance for a quantification of cell motion.** The moving variance of deflection signal recorded in HW (blue) and in FW (red) is shown in absence (top) and in presence (bottom) of cells, at three different time intervals: 60 ms (a), 300 ms (b) and 3 sec (c).*

To check the potential of the HWN sensors as a test of cancer malignancy the same experiment were performed with a less aggressive breast cancer cell line: the MCF-7. A comparison of the deflection signal of the cantilever before and after cell incubation (Fig. 7) showed that MDA-MB-231 moving cells (Fig. 7a) develop much higher forces than MCF-7 cells (Fig. 7b) when cultured on the HWN sensor. In order to associate the recorded forces to the cellular motion, the deflection measurements and time-lapse movie were recorded simultaneously (see Movie SM1 and SM2). We observed that the cells move on the cantilever and across the gaps. SEM images, acquired after measurements, confirmed the position of the cells on the sensors also indicating a strong adhesion that withstood washing and fixation procedures required by SEM sample preparation protocols (Fig. S4).

To quantify in a more rigorous way the forces developed by the cells, we performed the analysis of the variance over the entire measurement period. Indeed, the variance does not account for static deflection, while attributes the correct weight to rapid cell pulsations that would be lost by force averaging. To compare different measurements, it is necessary to consider the number and position of cells present on the cantilever, which, at this stage, are not under our control. By using fluorescence microscopy, we counted the number of cells on the cantilever and in the gaps (Fig. S5). In the analysis of variance, we classified the cantilevers according with the different number of cells adhering to the sensors: as expected the variance is larger when a larger number of cells adhered to the cantilever surface (Fig. 7c). The variance of MDA-MB-231 is much larger than that of MCF-7, suggesting that the former exert larger forces during, adhesion and motion process. This is consistent with data from the literature [36] and with the scratch wound assays, which showed that MDA-MB-231 have an higher mobility than MCF-7 cells (Fig. S6), which is consistent with their high potential ability to metastasize. These results indicate that the HWN sensor can be applied to detect variations in cell motility and distinguish highly motile cells from slow motile ones.

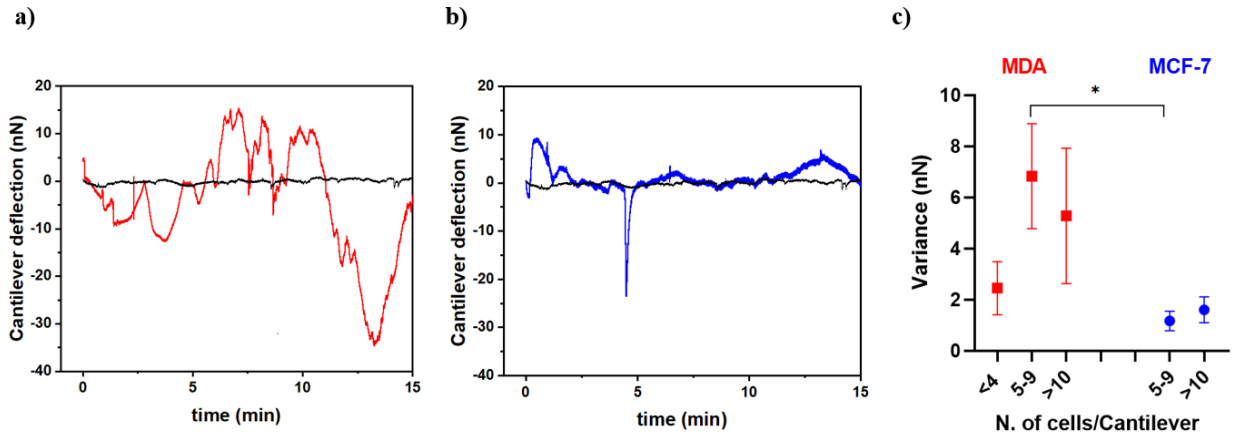

Figure 7: Cantilevers are sensitive to motility differences in different cell lines. *Deflection curves as function of time for bare cantilevers and in presence of MDA-MB 231 (a) or MCF7 cells (b) recorded in HW conditions. (c) Variance values obtained for the cantilevers L200 and 2 µm groove size grouped according to the number of cells adherent to the cantilever: for MD-MB231: 4 cells N=3; 5-9 cells N= 6; >10 cells N=4, for MCF7 5-7 cells N= 5; >10 cells N= 5. P-value: * (P<0.02).*

To further investigate the effect of cell positioning on force generation, we grouped the cantilever according to three different positions of cells (both MDA-MB-231 and MCF7) along the cantilever, as described in the scheme of Fig. 8a: 1) the majority of the cells lay in the apical region (>A); 2) the majority of the cells lay in the basal region (>B); 3) cells area equally distributed on the apical and on the basal region of the cantilever (A=B). The analysis of variance of the deflection signal showed significative larger values when most of the cells are in the apical zone (Fig. 8b). This result suggests that the apical zone may be the most sensitive zone of the cantilever, which in consistent with literature [33]. Indeed, two mechanisms could be addressed to explain the cantilever motion: change of surface tension at the cell-cantilever interfaces that caused a cantilever bending, which would be more effective when the cells are grown at the basal area, and traction forces exerted by the cells grown across the gap. In the latter, when cells are on the apical area, the forces required to deflect the cantilever are lower, with a sort of lever effect; on the other hand, when cells are at the basal area little changes in cell configuration would produce large cantilever deflection. The two effects sort of compensate each-other and as a first approximation we can assume that traction forces have the same effect not matter where the cells are grown. There is, however a third effect to be considered, the cantilever stiffening produced by cell adhesion [31],

which is stronger when cells are grown in the basal area, and alone could explain the results of figure 8, and in particular why A=B is not between >A and >B: the stiffening of cells at the basal area is the dominating effect. However, since the contribution of the cells across the gaps to the stiffness of the cantilever depends on their precise location and could affect in an unpredictable way the variance signal, further experiments in which cells position is predetermined are needed to draw a definitive conclusion on this aspect.

When the cells are evenly distributed on the apical and basal zones, the signal is lower than in the basal zone, suggesting that this positioning balances the system and reduces the detectable deflections.

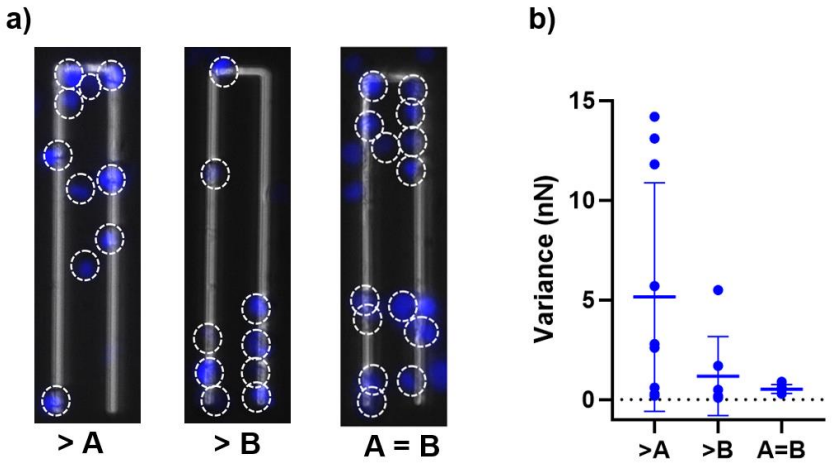

Figure 8: Cantilever response depend on the adhering cell position. *a) the fluorescence images of cantilevers (with a width of 30 µm, a gap of 2 µm, and 200 µm long) and cells as examples of arrangements of cells (MDA-MB-231) with three different combinations: a higher number of cells in the apical region (>A) or in the basal one (>B); an equal number of cells in the apical and basal zones (A=B). b) Analysis of variance (nN) of the oscillation signal as a function of the different cell positioning (MDA and MCF-7) on the HWN sensor.*

To compare the two cell lines, we also analyzed the variance as a function of the position of the cells in the apical or basal zone. We found that MDA-MB-231 cells had higher variance values, in both the apical and basal zones, than MCF-7 (Fig. 9). Finally, for the samples where most cells lay in the apical zone, we analyzed the variance for both MDA-MB-231 and MCF-7 as a function of the number of cells, finding, as expected, a linear correlation between variance amplitude and number of cells, indicating that by evaluating the variance we actually sum up the force contribution provided by every cell, even if they act randomly and independently.

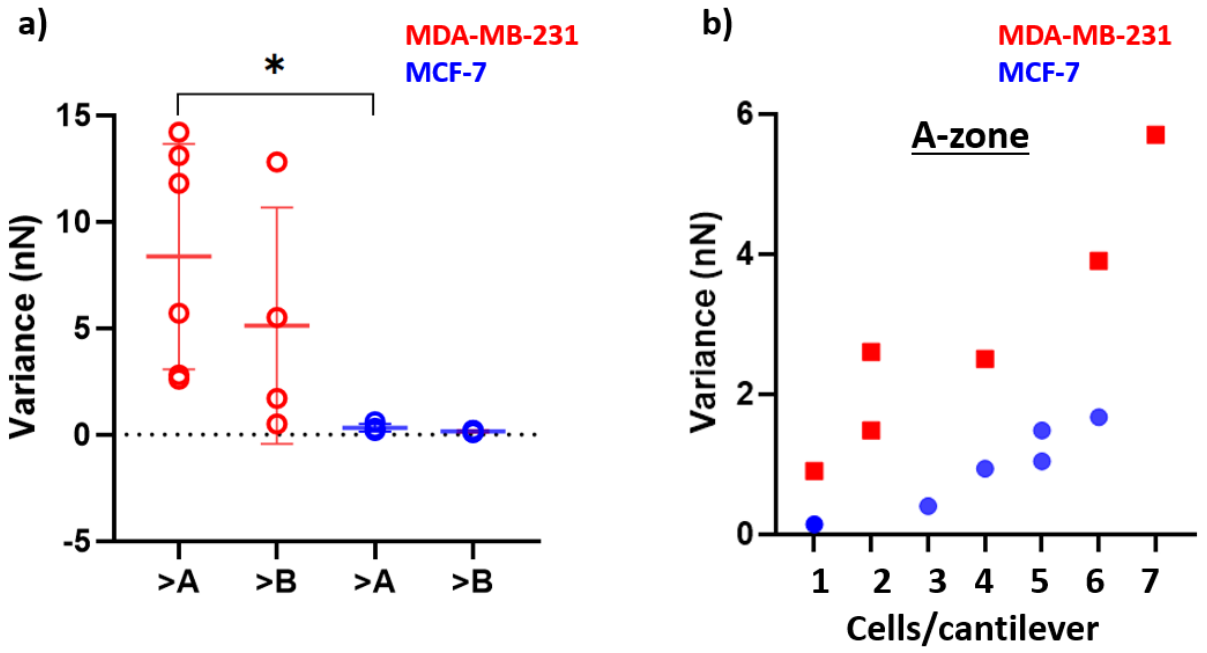

Figure 9: Cantilever response depend on the aggressivity and on the number of adhering cells *The variance analysis of oscillation signal in function of the cell lines (MDA-MB-231 or MCF-7). a) The MDA-MB-231 cells showed higher variance values both on the apical or basal zone if compared to MCF-7 ones; b) the analysis of variance for MDA-MB-231 and MCF-7 placed only on the apical zone (the most sensitive zone) showed higher values consistent with the number of cells. P-value: * (P<0.02).*

Upon further investigation of the forces exerted by the cells on the cantilever, we noticed that the deflection curves display macro- and micro-oscillations (see Fig. S3 and Materials and Methods). Both oscillations can be related to the cells adherent on the cantilever and moving on it or across the gap, exerting a contractile force that deforms the cantilever. The forces corresponding to these oscillations were evaluated and the results obtained for MDA-MB-231 and MCF-7 are compared in Fig. 10, where the cantilevers are grouped according to the number of cells. The force values obtained for macro- and micro-oscillations appear to be generally broadly distributed for MDA-MB231 compared to those observed for MCF7. The median force values for macro-oscillation of MDA-MB-231 are 1.8 nN for 4 cells, 0.96 nN for 5-9 cells, and 1.6 nN for > 10 cells; while for micro-oscillation, 2.3 nN for 4 cells, 1.3 nN for 5-9 cells, and 1.8 nN for > 10 cells were obtained. These median values for cantilevers with a number of more than 10 cells are lower for the MCF-7: macro-oscillations 0.65 nN for 5-9 cells, 0.40 nN > 10 cells and for micro-oscillations 1.0 nN for 5-9 cells, 0.79 nN for > 10 cells. These force values are compatible with those observed in

single cell adhesion measurements by Atomic Force Spectroscopy [37–40]. The evident, albeit not significative, decrease of average of forces with increasing number of cells can be explained recalling the dominating role of stiffening played by cells in the basal region. Indeed, cells exert force randomly in time, which very seldom are synchronized, while stiffening is a steady state process that definitely adds up: so the more the cells the lower the forces sensed by the cantilever. The widely dispersed force values for MDA-MB-231, especially for the micro-oscillations, could reflect a different mechanism of force transmission at the adhesion sites between the two cell lines, with a variation in cell spreading or even a different number of adhesion sites formed in the initial phase of adhesion, but this should be further investigated. These results suggest that HWN sensors could be a valuable tool for analyzing the force exerted by the cell during the adhesion or migration process and to monitor the effects of drug treatment on such processes in real-time.

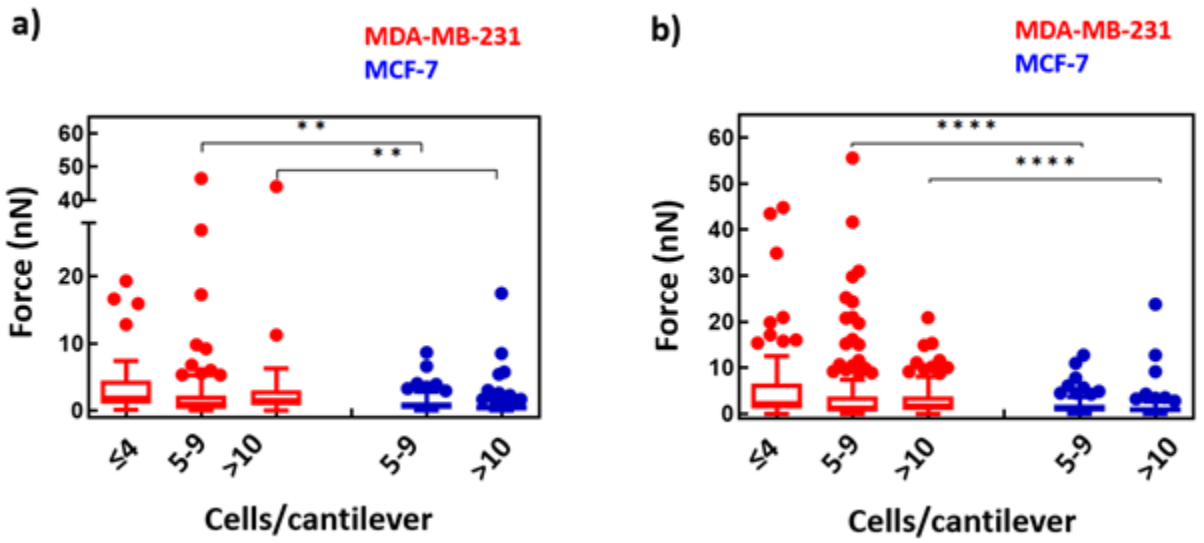

Figure 10: Cell forces depend on the cell aggressivity. *Forces correlated with the macro-oscillations (a) and micro-oscillations (b) obtained for MDA-MB-231 and MCF-7 grouped according to the number of cells adherent on the cantilever. P-value: ** (P<0.009), **** (P<0.0001).*

Conclusions

In summary, we have designed and fabricated a novel nano-motion detector that improves the sensitivity and performance of nano-motion systems and reduces the attenuation losses of the cantilever by operating with only one side in contact with the liquid solution. We showed that our approach allows to detect and evaluate the differences in cell motility and force developed during motion for cancer cell lines with different invasive characteristics.
These results suggest that our system may be a promising tool for real-time analysis of the dynamics of cell adhesion and the effect of drugs affecting this cellular process (i.e., adhesion or motility), opening the possibility of multiplexed platforms pushing toward monitoring therapeutic outcomes in cancer patients.

Acknowledgments

The authors gratefully acknowledge for the financial support the strategic project *Nano-Region Interreg V-A Italy-Slovenia 2014-2020.* This work was partially funded by the Italian Ministry of University and Research through the project *PRIN 2020 - Touch on a chip*.

References

[1] G. Binnig, C.F. Quate, Ch. Gerber, Atomic Force Microscope, Phys. Rev. Lett. 56 (1986) 930–933. https://doi.org/10.1103/PhysRevLett.56.930.

[2] A. Boisen, S. Dohn, S.S. Keller, S. Schmid, M. Tenje, Cantilever-like micromechanical sensors, Rep. Prog. Phys. 74 (2011) 036101. https://doi.org/10.1088/0034-4885/74/3/036101.

[3] M. Godin, V. Tabard-Cossa, Y. Miyahara, T. Monga, P.J. Williams, L.Y. Beaulieu, R.B. Lennox, P. Grutter, Cantilever-based sensing: the origin of surface stress and optimization strategies, Nanotechnology. 21 (2010) 075501. https://doi.org/10.1088/0957-4484/21/7/075501.

[4] S. Kasas, F.S. Ruggeri, C. Benadiba, C. Maillard, P. Stupar, H. Tournu, G. Dietler, G. Longo, Detecting nanoscale vibrations as signature of life, Proc. Natl. Acad. Sci. U. S. A. 112 (2015) 378–381. https://doi.org/10.1073/pnas.1415348112.

[5] A.C. Kohler, L. Venturelli, G. Longo, G. Dietler, S. Kasas, Nanomotion detection based on atomic force microscopy cantilevers, Cell Surf. 5 (2019) 100021. https://doi.org/10.1016/j.tcsw.2019.100021.

[6] G. Longo, L. Alonso-Sarduy, L.M. Rio, A. Bizzini, A. Trampuz, J. Notz, G. Dietler, S. Kasas, Rapid detection of bacterial resistance to antibiotics using AFM cantilevers as nanomechanical sensors, Nat. Nanotechnol. 8 (2013) 522–526. https://doi.org/10.1038/nnano.2013.120.

[7] P. Stupar, O. Opota, G. Longo, G. Prod'hom, G. Dietler, G. Greub, S. Kasas, Nanomechanical sensor applied to blood culture pellets: a fast approach to determine the antibiotic susceptibility against agents of bloodstream infections, Clin. Microbiol. Infect. Off. Publ. Eur. Soc. Clin. Microbiol. Infect. Dis. 23 (2017) 400–405. https://doi.org/10.1016/j.cmi.2016.12.028.

[8] S. Wu, Z. Zhang, X. Zhou, H. Liu, C. Xue, G. Zhao, Y. Cao, Q. Zhang, X. Wu, Nanomechanical sensors for direct and rapid characterization of sperm motility based on nanoscale vibrations, Nanoscale. 9 (2017) 18258–18267. https://doi.org/10.1039/C7NR03688D.

[9] H. Etayash, K. Jiang, S. Azmi, T. Thundat, K. Kaur, Real-time Detection of Breast Cancer Cells Using Peptide-functionalized Microcantilever Arrays, Sci. Rep. 5 (2015) 13967. https://doi.org/10.1038/srep13967.

[10] J. Fritz, M.K. Baller, H.P. Lang, H. Rothuizen, P. Vettiger, E. Meyer, H. Güntherodt, C. Gerber, J.K. Gimzewski, Translating biomolecular recognition into nanomechanics, Science. 288 (2000) 316–318. https://doi.org/10.1126/science.288.5464.316.

[11] P.S. Waggoner, H.G. Craighead, Micro- and nanomechanical sensors for environmental, chemical, and biological detection, Lab. Chip. 7 (2007) 1238–1255. https://doi.org/10.1039/B707401H.

[12] M. Melli, G. Scoles, M. Lazzarino, Fast Detection of Biomolecules in Diffusion-Limited Regime Using Micromechanical Pillars, ACS Nano. 5 (2011) 7928–7935. https://doi.org/10.1021/nn202224g.

[13] T.P. Burg, M. Godin, S.M. Knudsen, W. Shen, G. Carlson, J.S. Foster, K. Babcock, S.R. Manalis, Weighing of biomolecules, single cells and single nanoparticles in fluid, Nature. 446 (2007) 1066–1069. https://doi.org/10.1038/nature05741.

[14] J. Linden, E. Oesterschulze, Improving the quality factor of cantilevers in viscous fluids by the adaptation of their interface, Appl. Phys. Lett. 100 (2012) 113511. https://doi.org/10.1063/1.3694264.
[15] P. Peiker, S. Klingel, J. Menges, H.-J. Bart, E. Oesterschulze, A Partially Wettable Micromechanical Resonator for Chemical- and Biosensing in Solution, Procedia Eng. 168 (2016) 606–609. https://doi.org/10.1016/j.proeng.2016.11.225.
[16] S. Wu, X. Liu, X. Zhou, X.M. Liang, D. Gao, H. Liu, G. Zhao, Q. Zhang, X. Wu, Quantification of cell viability and rapid screening anti-cancer drug utilizing nanomechanical fluctuation, Biosens. Bioelectron. 77 (2016) 164–173. https://doi.org/10.1016/j.bios.2015.09.024.
[17] A perspective view on the nanomotion detection of living organisms and its features - Venturelli - 2020 - Journal of Molecular Recognition - Wiley Online Library, (n.d.). https://onlinelibrary.wiley.com/doi/10.1002/jmr.2849 (accessed October 24, 2021).
[18] S.K. Vashist, E. Lam, S. Hrapovic, K.B. Male, J.H.T. Luong, Immobilization of Antibodies and Enzymes on 3-Aminopropyltriethoxysilane-Functionalized Bioanalytical Platforms for Biosensors and Diagnostics, Chem. Rev. 114 (2014) 11083–11130. https://doi.org/10.1021/cr5000943.
[19] C.-P. Hsu, P.-Y. Hsu, Y.-L. Wu, W.-Y. Hsu, J.-J. Lin, Evolvement of cell–substrate interaction over time for cells cultivated on a 3-aminopropyltriethoxysilane (γ-APTES) modified silicon dioxide (SiO2) surface, Appl. Surf. Sci. 258 (2012) 8641–8648. https://doi.org/10.1016/j.apsusc.2012.05.066.
[20] R.F. Valentini, T.G. Vargo, J.A. Gardella, P. Aebischer, Patterned neuronal attachment and outgrowth on surface modified, electrically charged fluoropolymer substrates, J. Biomater. Sci. Polym. Ed. 5 (1993) 13–36. https://doi.org/10.1163/156856294x00626.
[21] A. Natarajan, C. Chun, J.J. Hickman, P. Molnar, Growth and electrophysiological properties of rat embryonic cardiomyocytes on hydroxyl- and carboxyl-modified surfaces, J. Biomater. Sci. Polym. Ed. 19 (2008) 1319–1331. https://doi.org/10.1163/156856208786052399.
[22] P. Saengdee, C. Promptmas, S. Thanapitak, A. Srisuwan, A. Pankiew, N. Thornyanadacha, W. Chaisriratanakul, E. Chaowicharat, W. Jeamsaksiri, Optimization of 3-aminopropyltriethoxysilane functionalization on silicon nitride surface for biomolecule immobilization, Talanta. 207 (2020) 120305. https://doi.org/10.1016/j.talanta.2019.120305.
[23] E. Ambrosetti, G. Bernardinelli, I. Hoffecker, L. Hartmanis, G. Kiriako, A. de Marco, R. Sandberg, B. Högberg, A.I. Teixeira, A DNA-nanoassembly-based approach to map membrane protein nanoenvironments, Nat. Nanotechnol. 16 (2021) 85–95. https://doi.org/10.1038/s41565-020-00785-0.
[24] E. Ambrosetti, M. Conti, A.I. Teixeira, S.D. Zilio, Patterned Carboxymethyl-Dextran Functionalized Surfaces Using Organic Mixed Monolayers for Biosensing Applications, ACS Appl. Bio Mater. 5 (2022) 3310–3319. https://doi.org/10.1021/acsabm.2c00311.
[25] J.L. Hutter, J. Bechhoefer, Calibration of atomic-force microscope tips, Rev. Sci. Instrum. 64 (1993) 1868–1873. https://doi.org/10.1063/1.1143970.
[26] K. Wagner, P. Cheng, D. Vezenov, Noncontact Method for Calibration of Lateral Forces in Scanning Force Microscopy, Langmuir. 27 (2011) 4635–4644. https://doi.org/10.1021/la1046172.

[27] F. Sumbul, N. Hassanpour, J. Rodriguez-Ramos, F. Rico, One-Step Calibration of AFM in Liquid, Front. Phys. 8 (2020). https://www.frontiersin.org/article/10.3389/fphy.2020.00301 (accessed January 18, 2022).
[28] M.J. Higgins, R. Proksch, J.E. Sader, M. Polcik, S. Mc Endoo, J.P. Cleveland, S.P. Jarvis, Noninvasive determination of optical lever sensitivity in atomic force microscopy, Rev. Sci. Instrum. 77 (2006) 013701. https://doi.org/10.1063/1.2162455.
[29] S. Dohn, W. Svendsen, A. Boisen, O. Hansen, Mass and position determination of attached particles on cantilever based mass sensors, Rev. Sci. Instrum. 78 (2007) 103303. https://doi.org/10.1063/1.2804074.
[30] B.N. Johnson, R. Mutharasan, Biosensing using dynamic-mode cantilever sensors: A review, Biosens. Bioelectron. 32 (2012) 1–18. https://doi.org/10.1016/j.bios.2011.10.054.
[31] J. Tamayo, P.M. Kosaka, J.J. Ruz, Á.S. Paulo, M. Calleja, Biosensors based on nanomechanical systems, Chem. Soc. Rev. 42 (2013) 1287–1311. https://doi.org/10.1039/C2CS35293A.
[32] M. Calleja, P.M. Kosaka, Á.S. Paulo, J. Tamayo, Challenges for nanomechanical sensors in biological detection, Nanoscale. 4 (2012) 4925–4938. https://doi.org/10.1039/C2NR31102J.
[33] B. Łabędź, A. Wańczyk, Z. Rajfur, Precise mass determination of single cell with cantilever-based microbiosensor system, PLoS ONE. 12 (2017) e0188388. https://doi.org/10.1371/journal.pone.0188388.
[34] D. Martínez-Martín, G. Fläschner, B. Gaub, S. Martin, R. Newton, C. Beerli, J. Mercer, C. Gerber, D.J. Müller, Inertial picobalance reveals fast mass fluctuations in mammalian cells, Nature. 550 (2017) 500–505. https://doi.org/10.1038/nature24288.
[35] C.-C. Chien, J. Jiang, B. Gong, T. Li, A. Gaitas, AFM Microfluidic Cantilevers as Weight Sensors for Single Cell Mass Measurements, (2022) 2022.02.21.481347. https://doi.org/10.1101/2022.02.21.481347.
[36] X.-X. Wu, G.G.-L. Yue, J.-R. Dong, C.W.-K. Lam, C.-K. Wong, M.-H. Qiu, C.B.-S. Lau, Actein Inhibits the Proliferation and Adhesion of Human Breast Cancer Cells and Suppresses Migration in vivo, Front. Pharmacol. 9 (2018). https://www.frontiersin.org/article/10.3389/fphar.2018.01466 (accessed February 9, 2022).
[37] L. Andolfi, E. Bourkoula, E. Migliorini, A. Palma, A. Pucer, M. Skrap, G. Scoles, A.P. Beltrami, D. Cesselli, M. Lazzarino, Investigation of Adhesion and Mechanical Properties of Human Glioma Cells by Single Cell Force Spectroscopy and Atomic Force Microscopy, PLOS ONE. 9 (2014) e112582. https://doi.org/10.1371/journal.pone.0112582.
[38] E. Migliorini, J. Ban, G. Grenci, L. Andolfi, A. Pozzato, M. Tormen, V. Torre, M. Lazzarino, Nanomechanics controls neuronal precursors adhesion and differentiation, Biotechnol. Bioeng. 110 (2013) 2301–2310. https://doi.org/10.1002/bit.24880.
[39] L. Andolfi, A. Murello, D. Cassese, J. Ban, S.D. Zilio, M. Lazzarino, High aspect ratio silicon nanowires control fibroblast adhesion and cytoskeleton organization, Nanotechnology. 28 (2017) 155102. https://doi.org/10.1088/1361-6528/aa5f3a.
[40] P. Bertoncini, S. Le Chevalier, S. Lavenus, P. Layrolle, G. Louarn, Early adhesion of human mesenchymal stem cells on TiO(2) surfaces studied by single-cell force spectroscopy measurements, J. Mol. Recognit. JMR. 25 (2012) 262–269. https://doi.org/10.1002/jmr.2193.